[CANCER RESEARCH 63, 86–92, January 1, 2003]

Doxorubicin-loaded Fab′ Fragments of Anti-disialoganglioside Immunoliposomes Selectively Inhibit the Growth and Dissemination of Human Neuroblastoma in Nude Mice[1]

Fabio Pastorino,[2] Chiara Brignole,[2] Danilo Marimpietri, Puja Sapra, Elaine H. Moase, Theresa M. Allen, and Mirco Ponzoni[3]

Differentiation Therapy Unit, Laboratory of Oncology, G. Gaslini Children's Hospital, Genoa, Italy 16148 [F. P., C. B., D. M., M. P.], and Department of Pharmacology, University of Alberta, Edmonton, Alberta, Canada T6G2H7 [P. S., E. H. M., T. M. A.]

ABSTRACT

Neuroblastoma (NB) is the most common extracranial solid tumor in children. Intensive therapeutic intervention does not prolong the overall disease-free survival rate for this tumor. NB tumor, but not normal tissues, overexpress the disialoganglioside (GD_2) at the cell surface. Anti-GD_2 whole antibodies (aGD_2) or their corresponding Fab′ fragments were covalently coupled to Stealth immunoliposomes (aGD_2-SIL or Fab′-SIL), and their binding to GD_2-positive NB cells was measured. Cytotoxic effects of immunoliposomes loaded with doxorubicin (DXR) were determined. Radiolabelled immunoliposomes were used to evaluate pharmacokinetics (PK). The effectiveness of different liposomal formulations of DXR was tested against a metastatic model of human NB in nude mice. aGD_2-SIL and Fab′-SIL showed concentration-dependent specific binding and uptake by GD_2-positive NB cells. DXR entrapped in aGD_2-SIL or Fab′-SIL (aGD_2-SIL[DXR], Fab′-SIL[DXR]) showed higher cytotoxicities than nontargeted liposomes (SL[DXR]). DXR-loaded Fab′-SIL (Fab′-SIL[DXR]) also showed specific binding, uptake, and cytotoxic effects on several GD_2-positive NB cells *in vitro*. PK studies showed that Fab′-SIL had long-circulating profiles in blood compared with aGD_2-SIL, with the PK profile for Fab′-SIL being almost identical to that obtained with nontargeted Stealth liposomes. *In vivo*, long-term survivors were obtained in mice treated with Fab′-SIL[DXR] but not in untreated animals, or those treated with free aGD_2 Fab′, Fab′-SIL (no drug), free-DXR, or nontargeted Stealth liposomes[DXR] (no antibody; $P < 0.0001$). Immunoliposomes containing DXR prevented the establishment and growth of the tumor in all of the organs examined. In conclusion, Fab′-SIL[DXR] formulations led to the total inhibition of metastatic growth of human NB in a nude mouse metastatic model. This formulation should receive clinical evaluation as adjuvant therapy of NB.

INTRODUCTION

The effective treatment of NB,[4] one of the most common solid tumors in children (1), either at advanced stages or at minimal residual disease, remains one of the major challenges in pediatric oncology. Prognosis for patients with this disease has improved with advances in medical care, but the overall 5-year survival is still <60% (2). However, the use of intensive therapeutic interventions have marginally prolonged the overall long-term disease-free survival rates, mainly because of the dose-limiting toxicity associated with systemic delivery of cytotoxic drugs *in vivo*. Indeed, the incidence of fatal relapses is still high, and long-term survival remains very low (3). Thus, innovative therapies are required to eradicate residual disease after chemotherapy and surgery.

NB is a chemosensitive tumor and cytotoxic agents such as DXR are considered to be important and effective treatment modalities. However, the therapeutic efficacy of this anticancer drug, which is widely used in the treatment of solid tumors, is restricted by dose-limiting toxicity to bone marrow and heart tissue (4). The selective toxicity of DXR would be greatly improved if the concentration of drug in tumors could be increased relative to that in sensitive normal tissues. NB cells express abundant amounts of the disialoganglioside GD_2 at their cell surface, but the presence of this epitope on normal tissues, such as the cerebellum and peripheral nerves, is limited (5–8).

In the last few years, liposomes have been used to increase the selective toxicity of chemotherapy drugs, resulting in improved therapeutic outcomes and/or reduced toxicities (9–11). A long circulating (sterically stabilized or Stealth) liposomal formulation of DXR (Doxil/Caelyx) has been approved for use in the treatment of both Kaposi's sarcoma and ovarian cancer (12, 13). In patients receiving large cumulative doses of DXR, clinical cardiotoxicity was reduced (14), and this liposomal formulation of DXR is now under advanced clinical trial evaluation for several human solid cancers.

We reported previously that the ability to selectively target liposomal anticancer drugs via specific ligands against antigens expressed on malignant cells could improve the antitumor activity of the liposomal formulations. Several studies have shown that the use of immunoliposomes (SIL) significantly increased target cell binding *in vitro* (15–19) and improved therapeutic efficacy *in vivo* (16, 20–22). Moreover, the coupling antibody Fab′ fragments instead of whole immunoglobulin molecules to Stealth liposomes have increased their circulation times (23) and improved their *in vivo* efficacy (24). Because NB tumors express abundant amounts of GD_2 at the cell surface, and because this epitope is only minimally expressed by normal tissues (5, 6), the use of anti-GD_2 as a ligand for targeting liposomal DXR to NB merits additional investigation.

In this study we examined target binding and selective cytotoxicity of aGD_2-targeted formulations against GD_2-positive NB cell lines *in vitro*. Pharmacokinetic studies were performed, and survival times were evaluated in nude mice xenografts of the human NB cell line, HTLA-230. The HTLA-230 cells, when administered i.v. in nude mice, provide an *in vivo* pseudometastatic model for the metastatic spread of tumor in human disease (25). Our results clearly show that liposomal DXR targeted via Fab′ fragments of aGD_2 were effective in suppressing the growth of metastases in mice implanted with a human NB tumor.

Received 7/8/02; accepted 10/28/02.

The costs of publication of this article were defrayed in part by the payment of page charges. This article must therefore be hereby marked *advertisement* in accordance with 18 U.S.C. Section 1734 solely to indicate this fact.

[1] Supported by Fondazione Italiana per la lotta al Neuroblastoma, Costa Crociere, and Associazione Italiana Ricerca Cancro (AIRC). F. P. is a recipient of a Fondazione Italiana per la lotta al Neuroblastoma fellowship.

[2] These authors contributed equally to the work.

[3] To whom requests for reprints should be addressed, at Differentiation Therapy Unit, Laboratory of Oncology, G. Gaslini Children's Hospital, Largo G. Gaslini 5, 16148 Genoa, Italy. Phone: 39-010-5636342; Fax: 39-010-3779820; E-mail: mircoponzoni@ospedale-gaslini.ge.it.

[4] The abbreviations used are: NB, neuroblastoma; DXR, doxorubicin; SIL, sterically stabilized (Stealth) immunoliposome; SL, nontargeted Stealth liposome; CI, confidence interval; SL[DXR], DXR-loaded SL; DSPE, distearoylphosphatidylethanolamine; PEG, polyethylene glycol; mAb, monoclonal antibody; aGD_2, anti-GD_2 whole murine monoclonal antibody; HSPC, hydrogenated soy phosphatidylcholine; FACS, fluorescence-activated cell sorter; Fab′, Fab′ fragments of aGD_2; aGD_2-SIL[DXR], DXR-loaded aGD_2-targeted sterically stabilized (Stealth) immunoliposome; Fab′-SIL[DXR], DXR-loaded Fab′ fragments of aGD_2-targeted sterically stabilized (Stealth) immunoliposome; MRT, mean residence time; CHOL, cholesterol; [^{3}H]CHE, cholesteryl-[1,2-^{3}H-(N)]-hexadecyl ether; TI, [^{125}I]-tyraminylinulin.

MATERIALS AND METHODS

Chemicals and mAbs. HSPC and methoxy poly (ethyleneglycol; Mw 2000) covalently linked to distearoylphosphatidylethanolamine were generous gifts from ALZA, Corp. (Menlo Park, CA). Maleimide-terminated polyethylene glycol-DSPE was purchased from Shearwater Polymers, Inc. (Huntsville, AL). CHOL was purchased from Avanti Polar Lipids (Alabaster, AL). [^{3}H]CHE and Na^{125}I were purchased from New England Nuclear (Mississauga, Ontario, Canada). DXR (Adriamycin RDF) was obtained from Adria Laboratories Inc. (Mississauga, Ontario, Canada) or purchased from Sigma Chemical Co. (St. Louis, MO). The hybridoma 14G.2a, which secretes a murine IgG2a mAb specific for the GD_2 antigen, was a generous gift of Ralph A. Reisfeld (The Scripps Institute, La Jolla, CA; Ref. 26). The murine mAb anti-CD19 (IgG2a) was produced from the FMC-63 hybridoma obtained from Dr. Heddy Zola (Child Health Research Institute, Adelaide, Australia).

For preparation of $F(ab')_2$ fragments, purified antibody was digested with lysyl endopeptidase (Wako Chemicals, Richmond, VA) in 50 mM Tris-HCl (pH 8.5) at 37°C for 3 h, and the reaction mix was passed through a protein-A/G column equilibrated with 50 mM Tris-HCl (pH 7.5). $F(ab')_2$ fragments were reduced with 7.5 mM β-mercaptoethylamine (Sigma) for 90 min at 37°C in acetate buffer (pH 6.5), after which the reducing agent was removed by passing the sample over a Sephadex G-25 column chromatography pre-equilibrated with the same buffer. The concentration of all of the mAbs was determined by spectrophotometry ($\lambda = 280$ nm), and purity was assessed by SDS-PAGE. The reactivities of whole mAbs, $F(ab')_2$, and Fab′ fragments were checked by indirect immunofluorescence using FITC-labeled goat antimouse antibody and IgG-Fab′-specific (Sigma), respectively, and FACS analysis (Becton Dickinson, San Jose, CA).

Liposome Preparation and DXR Loading. SLs and SILs were synthesized from HSPC:CHOL:DSPE-PEG_{2000}, 2:1:0.1 molar ratio, and HSPC:CHOL:DSPE-PEG_{2000}:DSPE-PEG_{2000}-MAL, 2:1:0.08:0.02 molar ratio, respectively. The lipids were first dissolved in chloroform and then combined in the appropriate ratios (15, 19, 27). In some preparations, [^{3}H]CHE was added as a nonexchangeable, nonmetabolizable lipid tracer. After evaporation under nitrogen, dried lipid films were hydrated in 25 mM HEPES and 140 mM NaCl buffer (pH 7.4). The hydrated liposomes were sequentially extruded at 65°C (Lipex Biomembranes Extruder, Vancouver, British Columbia, Canada) through a series of polycarbonate filters of pore size ranging from 0.2 μm down to 0.08 μm to produce primarily unilamellar vesicles. Liposomal size was characterized by dynamic light scattering (28) using a Brookhaven BI90 submicron particle size analyzer (Brookhaven Instruments Corp., Holtsville, NY). The mean liposomal diameters of extruded liposomes were in the range of 98–110 nm.

DXR was loaded into liposomes via an ammonium sulfate gradient, using a method adapted from Ref. 29 and reported previously (21). The loading efficiency of DXR was >95%, and liposomes routinely contained DXR at a concentration of 150–180 μg DXR/μmol phospholipids (PL).

For preparation of immunoliposomes, whole mAb or Fab′ fragments, trace labeled with ^{125}I (21), were coupled to the maleimide terminus of maleimide-terminated polyethylene glycol-DSPE, as described previously (19). After activation with Traut's reagent (2-iminothiolane) at a molar ratio of 20:1 (Traut's: IgG) for 1 h at room temperature in HEPES buffer (pH 8.0; 25 mM HEPES and 140 mM NaCl), unreacted Traut's reagent was removed using a G50 column. The coupling reaction was run at molar ratio of whole mAb or Fab′ fragments to phospholipid molar ratio of 1:2000 or 1:1000, respectively, under argon atmosphere for 18 h at room temperature. Uncoupled mAb or Fab′ were separated from the liposomes by passing the coupling mixture through a Sepharose CL-4B column in HEPES buffer (pH 7.4). The efficiency of coupling was determined from the amount of ^{125}I-labeled mAb or Fab′ bound to the surface of liposomes and is expressed as nmol mAb/μmol PL. The coupling densities on liposomes were in the range of 0.33–0.53 nmol anti-GD_2 mAb/μmol PL (0.66–1.06 nmol binding sites, because each mAb has two binding sites) and 0.54–0.91 nmol anti-GD_2 Fab′ fragments/μmol PL.

Cell Lines and Culture Condition. To broadly cover the phenotypes exhibited by NB cells *in vitro*, we used the GD_2-positive human NB cell lines ACN, GI-LI-N, HTLA-230, and IMR-32 (17, 19). Four GD_2-negative cell lines, the adherent cell lines HeLa (human cervical carcinoma) and A431 (human epidermoid carcinoma), and the suspension cell lines HL-60 (human myeloid leukemia) and Jurkat (human T cell) were used in some experiments as controls. All of the cell lines were grown in RPMI 1640 supplemented with 10% fetal bovine serum, 50 IU/ml sodium penicillin G, 50 μg/ml streptomycin sulfate, and 2 mM L-glutamine, as described previously (30).

Cellular Association Studies. ^{3}H[CHE]-labeled liposomes were used to measure cellular binding and uptake, as described previously (17, 19). Briefly, cells (1×10^6/ml) were plated in 48-well tissue culture plates. Different formulations of [^{3}H]CHE-labeled liposomes, with or without coupled aGD_2-specific mAb or isotype-matched nonspecific mAb, anti-CD19, were added to each well (100–800 nmol PL/ml) and maintained at either 4°C or 37°C in a total volume of 200 μl. In competition experiments, a 25-fold excess of free mAb aGD_2 was added 30 min before adding [^{3}H]CHE-labeled immunoliposomes. After a 1-h incubation, the cells were extensively washed, trypsinized, and lysed with 1 N NaOH for protein evaluation and analyzed in a scintillation counter.

The cellular association with NB cells of immunoliposomes targeted via either aGD_2 or Fab′-fragments was also analyzed by flow cytometry (FACS). Aliquots of cells (1×10^6/tube) were incubated for 1 h at 4°C or 37°C with different formulations of liposomes (SL, aGD_2-SIL, or Fab′-SIL). The cells were washed subsequently with PBS, and then incubated with goat antimouse FITC-conjugated IgG-Fab′ specific for 30 min at 4°C, and, after washing, were enumerated by flow cytometry. All of the cytometry experiments were performed using a FACScan instrument for fluorescence-activated cell sorting (Becton-Dickinson Immunocytometry Systems).

***In Vitro* Cytotoxicity Experiments.** The specific inhibition of the proliferation of NB cells was determined by an *in vitro* proliferation assay using 3-(4,5-dimethylthiazol-2-yl)-2,5-diphenyltetrazolium bromide (31). Samples included free DXR and SL[DXR], aGD_2-SIL[DXR], or Fab′-SIL[DXR]. Briefly, 3×10^4 HTLA-230 or GI-LI-N NB cells (100% and 70% GD_2-positive, respectively) were plated in 96-well plates and incubated with either free DXR or liposome-encapsulated DXR as above, for 1, 24, and 48 h at 37°C. At the different time points, the cells were washed twice with PBS before replacing with fresh medium and incubating for an additional 71, 48, and 24 h, respectively, *i.e.*, all of the plates were incubated for a total time of 72 h. At the end of the incubation, tetrazolium dye was added, plates were incubated for an additional 3–4 h, formazan crystal were dissolved in acid isopropanol, and then the plates were read on a Titertek Multiskan Plus (Flow Laboratories, Inc., Mississauga, Ontario, Canada) at the dual wavelengths of 570 and 650 nm (31).

Leakage of DXR from Liposomes. Release of DXR from liposomes was measured by incubation of DXR-containing liposomes at 37°C with either PBS or human plasma in 24-well plates at a final DXR concentration of 10 μg/ml, as described previously (32). DXR leakage from liposomes was followed by measuring the fluorescence dequenching of DXR at selected time points (0–24 h) using fluorimetry (33). Complete release (100% dequenching) of DXR was obtained by treating liposomes with 5 μl of 10% Triton X-100 in distilled water/ml. The percentage of DXR released was determined from fluorescence intensity of wells relative to 100% dequenching.

Pharmacokinetic Experiments. Six to 8-week-old outbred female BALB/c mice were purchased from the Health Sciences Laboratory Animal Services, University of Alberta. BALB/c mice in the weight range of 20–30 g were injected via the tail vein with a single dose of liposomes (0.5 μmol PL/mouse), with or without coupled aGD_2 or GD_2 Fab′ fragments, containing approximately $2–4 \times 10^5$ cpm of the aqueous-space marker TI (34). At selected time points (0.5, 2, 6, 12, 24, and 48 h) postinjection, mice (3 mice/group) were anesthetized with halothane and sacrificed by cervical dislocation. A blood sample (100 μl) was collected by heart puncture and counted for the ^{125}I label in a Beckmann 8000 gamma counter. Blood correction factors were applied to all of the samples (35). Pharmacokinetic parameters were calculated using the software package PKAnalyst, Version 1.1 (MicroMath Scientific Software, Salt Lake City, UT). In these experiments and the experiments, below, all of the procedures involving animals and their care were in accordance with institutional guidelines, and in compliance with national and international laws and policies.

***In Vivo* Therapeutic Studies.** Four to 6-week-old female athymic nude (*nu/nu*) mice were purchased from Harlan Laboratories (Harlan Italy-S. Pietro al Natisone, UD). Female nude mice (8 mice/group) were injected with HTLA-230 cells (3.5×10^6 cells in 200 μl of HEPES-buffered saline) in the tail vein (i.v.) on day 0, and treated on days 1, 3, 5, and 7 postinoculation of cells at a dose of 2.5 mg DXR/kg (schedule A). In an alternative dosing

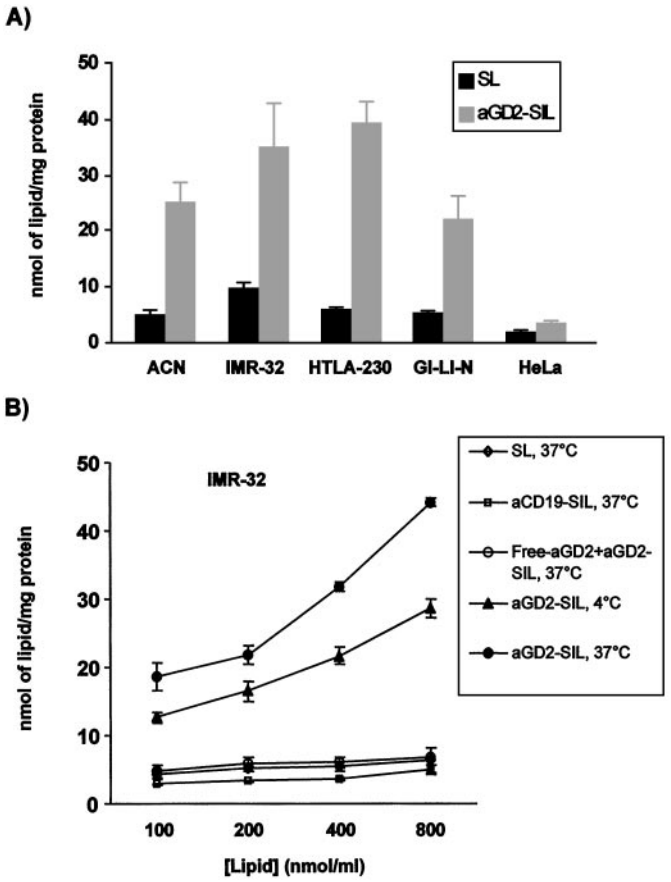

Fig. 1. *A*, cellular association at 37°C of [^{3}H]CHE-labeled targeted (*aGD$_2$-SIL*) and nontargeted (*SL*) liposomes to GD$_2$-positive NB cell lines, ACN, IMR-32, HTLA-230 and GI-LI-N, and control, GD$_2$-negative cells, HeLa. Liposomes were incubated with 1×10^6 cells at 400 nmol phospholipid/ml. *B*, cellular association (binding and uptake) to IMR-32 cells of aGD$_2$ immunoliposomes as a function of lipid concentration. Liposomes (100–800 nmol phospholipid/ml) were incubated with 1×10^6 cells at 37°C for 1 h: SL (◇), nonspecific aCD19-SIL (□), and aGD$_2$-SIL (●). Cells were also incubated at 4°C for 1 h with aGD$_2$-SIL (▲). In competition experiments, cell association of aGD$_2$-SIL was conducted in the presence of excess free-aGD$_2$ (○). Data are expressed as nmol of PL/mg protein, and are the mean of four experiments, each done in triplicate ±CI.

schedule, mice were injected with 4×10^6 HTLA-230 cells on day 0, and treated on days 1 and 3 postinoculation of cells at a dose of 5 mg DXR/kg (schedule B). For each experiments, mice received one of the following treatments: HEPES-buffered saline, free Fab′ from aGD$_2$ (amount of Fab′ was equivalent to the amount coupled to the injected dose of Fab′-SIL[DXR]), Fab′-SIL, SL[DXR], or Fab′-SIL[DXR]. In another experiment mice received a single administration of 10 mg of Fab′-SIL[DXR]/kg on day 1 postinoculation of cells. Mice were monitored routinely for weight loss, and survival times were used as the main criterion for determining treatment efficacy. Histological evaluation of microscopic metastases was performed for all of the tissues. Organs were fixed in neutral-buffered 10% formalin, processed by standard methods, embedded in paraffin, sectioned at 5–10 μm, and stained with H&E.

Statistical Methods. Results are expressed as means ±95% CIs. All of the *in vitro* data derive from at least three independent experiments. All of the *in vivo* experiments have been performed at least twice with similar results. The significance of the differences between experimental groups in the survival experiments was determined by Kaplan-Meier curves and Peto's log-rank test by the use of StatsDirect statistical software (CamCode, Ashwell, United Kingdom).

RESULTS

Cellular Association and Uptake of aGD$_2$-targeted Immunoliposomes. We studied the levels of cellular association of [^{3}H]CHE-labeled aGD$_2$-targeted or nontargeted liposomes to four GD$_2$-positive human NB cell lines (GI-LI-N, ACN, HTLA-230, and IMR-32) and four GD$_2$-negative cell lines (HeLa; Fig. 1*A*), A431, HL-60, and Jurkat (data not shown). The data showed that the level of cellular binding of liposomes is dependent on GD$_2$ expression in the different cell lines. aGD$_2$-SIL showed 5–10 times higher cellular association to all of the GD$_2$-positive cell lines, compared with nontargeted liposomal preparations (SL). In contrast, the GD$_2$-negative cell line, HeLa, showed very low levels of liposomes associated with the cells for both targeted or nontargeted formulations (Fig. 1*A*).

To examine whether immunoliposomes (aGD$_2$-SIL) could be specifically taken up by the GD$_2$-expressing NB cells, IMR-32, *in vitro* binding studies were performed at 4°C and 37°C (Fig. 1*B*). aGD$_2$-SIL increased the cell association on IMR-32 cells by a factor of 10-fold over that obtained with liposomes bearing nonspecific isotype-matched antibodies (*e.g.*, aCD19) or with mAb-free liposomes when incubated at 37°C and by a factor of 5-fold when incubated at 4°C. These results suggest that internalization of aGD$_2$-SIL may be occurring at 37°C. Moreover, in competition experiments we showed that the dose-dependent cellular association and uptake of the aGD$_2$-targeted liposomes to GD$_2$-positive NB cells could be blocked by the addition of a 25-fold excess of free mAb 30 min before adding [^{3}H]CHE-labeled aGD$_2$-SIL (Fig. 1*B*).

***In Vitro* Cytotoxicity Experiments.** The cytotoxicity of DXR, either free or encapsulated in SL[DXR] (no mAb) or aGD$_2$-SIL[DXR], was compared as a function of time. As expected (Table 1), the IC$_{50}$ decreased as the exposure of cells to drug increased from 1 h to 48 h. After 24 h of incubation aGD$_2$-SIL[DXR] were ~3-fold more cytotoxic than SL[DXR] against GI-LI-N cells and 4-fold more cytotoxic against HTLA-230 cells, respectively. Similar cytotoxicities were seen against HeLa cells for SL[DXR] and aGD$_2$-SIL[DXR] suggesting that binding and internalization of the targeted liposomes to the GD$_2$ epitope in the other cell lines is contributing to the increased cytotoxicity. Free DXR had the highest levels of cytotoxicity against all three of the cell lines *in vitro*, and did not distinguish between GD$_2$-expressing and GD$_2$-nonexpressing cell lines (Table 1). With increased exposure times, the IC$_{50}$ for the aGD$_2$-SIL[DXR] became more similar to that of free DXR for the GD$_2$-expressing cells but not for the HeLa cells. This suggests that a longer exposure of aGD$_2$-SIL[DXR] to GD$_2$-positive cells increases the cellular uptake of the liposomal drug package, contributing to the increased cytotoxicity. Because free DXR is rapidly and widely redistributed to tissues after *in vivo* administration, it is expected that the targeted formulations, with their ability to selectively bind the target cells, will have an advantage over the free drug *in vivo*.

All of the liposomal formulations showed minimal leakage in PBS,

Table 1 *Cytotoxicity of various formulations of DXR against GD$_2$-positive (GI-LI-N and HTLA-230) and GD$_2$-negative (HeLa) cells*

Cell lines	Free-DXR	SL[DXR]	aGD$_2$-SIL[DXR]	Fab′-SIL[DXR]
	IC$_{50}$ (μM) ± SD[a]			
GI-LI-N				
1 h	2.7 ± 0.2	>300	109.3 ± 2.4	97.0 ± 3.7
24 h	0.4 ± 0.2	12.6 ± 0.4	4.9 ± 0.2	ND[b]
48 h	0.2 ± 0.1	4.9 ± 0.4	1.5 ± 0.1	ND
HTLA-230				
1 h	2.6 ± 0.3	93.9 ± 4.0	22.6 ± 6.9	24.0 ± 1.5
24 h	0.6 ± 0.1	8.5 ± 0.6	2.1 ± 0.8	ND
48 h	0.5 ± 0.1	6.8 ± 0.9	1.7 ± 0.4	ND
HeLa				
1 h	3.2 ± 0.3	>300	>300	>300
24 h	1.2 ± 0.1	197.8 ± 0.5	194.4 ± 2.1	ND
48 h	0.6 ± 0.1	50.5 ± 0.2	50.3 ± 0.4	ND

[a] IC$_{50}$ was evaluated as dose-response inhibition of MTT assay. Data are means ± SD of three independent experiments each done in triplicate.
[b] ND, not determined.

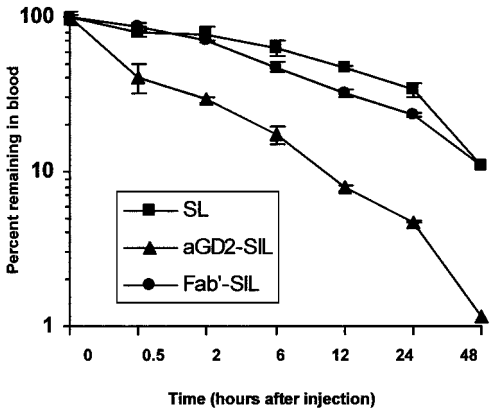

Fig. 2. Blood clearance kinetics of SL, aGD$_2$-SIL, and Fab′-SIL in BALB/c mice. Liposomes were labeled with the aqueous-space label TI and were injected i.v. in a single bolus dose (0.5 μmol PL/mouse). Treatment groups consisted of Fab′-SIL (●), aGD$_2$-SIL (▲), and SL (■). At different times postinjection blood was collected and counted for ^{125}I label. Each point represents the average of 3 mice, ±CI.

retaining >90% of the encapsulated DXR after 24 h of incubation. As expected from our previous data (31), when leakage experiments were conducted in 25% human plasma, liposomes showed a slow DXR leakage (12%) at 24 h. Hence, it appears likely that the cytotoxicity results for the aGD$_2$-SIL[DXR] were not attributable to a significant extent on the release of drug from the formulations and uptake of the released drug.

Pharmacokinetic Profiles. The pharmacokinetics of TI-labeled SL, aGD$_2$-SIL, and Fab′-SIL was evaluated in 6–8-week old outbred female BALB/c mice (34). In Fig. 2, the results are expressed as percentage of the administered dose remaining in blood, which corrects for leakage of the label, and represents intact liposomes at selected time points (36, 37). These findings clearly indicate that liposomes coupled to Fab′ fragments of aGD$_2$ had long-circulating profiles in blood with a MRT of 26.2 h, compared with aGD$_2$-SIL (MRT of 9.5 h) with the PK profile for Fab′-SIL being almost identical to that obtained with SL (MRT of 26.2 h).

***In Vivo* Therapeutic Studies.** In preliminary *in vivo* experiments[5] free mAb aGD$_2$ showed an immunotherapeutic effect via Fc receptor-mediated mechanisms with subsequent activation of antibody-dependent cellular cytotoxicity and complement-depended cytotoxicity, confirming previous reports (7, 8, 38). Thus, to obtain therapeutic effects attributable only to the cytotoxic effects of targeted DXR, we decided to couple the Fab′ portion of aGD$_2$ to the liposomes. To determine whether Fab′-SIL maintained the specific cellular association for GD$_2$-positive cell lines, HTLA-230 cells were incubated with SL, aGD$_2$-SIL, or Fab′-SIL for 1 h and analyzed by flow cytometry. Fab′-SIL (Fig. 3, *bold line*) showed high levels of binding to the HTLA-230 cell line, similar to that obtained with aGD$_2$-SIL (Fig. 3, *thin line*), whereas SL did not bind to NB cells (Fig. 3). The GD$_2$-negative cell line HeLa showed no differences in cell association among SL, aGD$_2$-SIL, or Fab′-SIL, additionally confirming the selective cell association of Fab′-SIL to GD$_2$-positive cells (Fig. 3). To confirm these results, [^{3}H]CHE-labeled Fab′-SIL were also used in some cell binding experiments. Fab′-SIL showed 10-fold higher levels of both cellular binding and internalization to NB cells over that obtained with liposomes bearing nonspecific isotype-matched Fab′-fragments or with Fab′-fragment-free liposomes (data not shown).

The cytotoxic effects of DXR encapsulated in Fab′-SIL (Fab′-SIL[DXR]) were evaluated. Fab′-targeted liposomal DXR formulations showed higher cytotoxicities against GI-LI-N and HTLA-230 cells compared with SL[DXR] (see Table 1). After a 1-h incubation the IC$_{50}$ was similar for the Fab′-SIL to those seen for the aGD$_2$-SIL[DXR] (Table 1).

To evaluate the *in vivo* effectiveness of Fab′-SIL[DXR], experiments were performed using two different dosing protocols, keeping in mind that the commonly used dosing of DXR in nude mice with human xenografts is 2.5–10 mg/kg mouse/week (39). The results are summarized in Fig. 4. For schedule A (2.5 mg/kg DXR on days 1, 3, 5, and 7), mice receiving Fab′-SIL[DXR] showed a significant improvement ($P = 0.0003$) in long-term survivors compared with all of the other groups. Seven of 8 mice treated with Fab′-SIL[DXR] were still alive at 120 days after inoculation of tumor cells (Fig. 4*A*). Mice receiving schedule A also showed partial, but not statistically significant ($P = 0.6$), improvement in mean survival times for mice treated with SL[DXR] (Fig. 4*A*) when compared with untreated animals or mice treated with free-aGD$_2$ Fab′, Fab′-SIL, and free-DXR. In addition, histological evaluation of the main organs clearly showed that

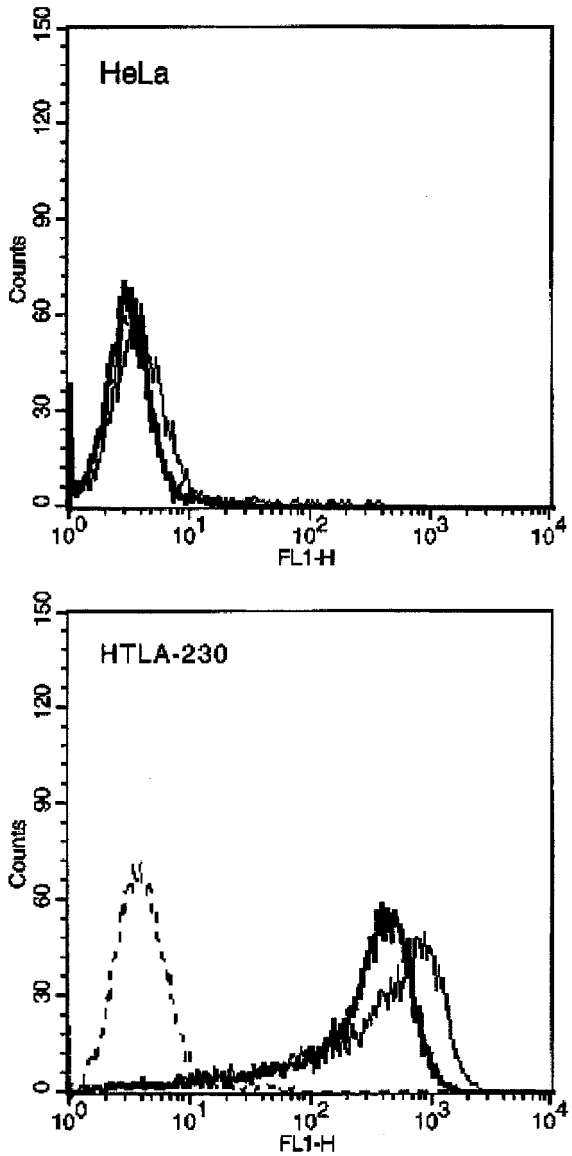

Fig. 3. Cellular association of immunoliposomes with NB cells analyzed by flow cytometry. One × 10^6 cells/tube were incubated for 1 h at 4°C with SL, aGD$_2$-SIL, or Fab′-SIL, followed by goat antimouse FITC-conjugated IgG specific for Fab′ for 30 min at 4°C. After washing, the cells were enumerated by FACS. SL, *dotted line*; aGD$_2$-SIL, *thin line*; Fab′-SIL, *bold line*.

[5] F. Pastorino, personal observation.

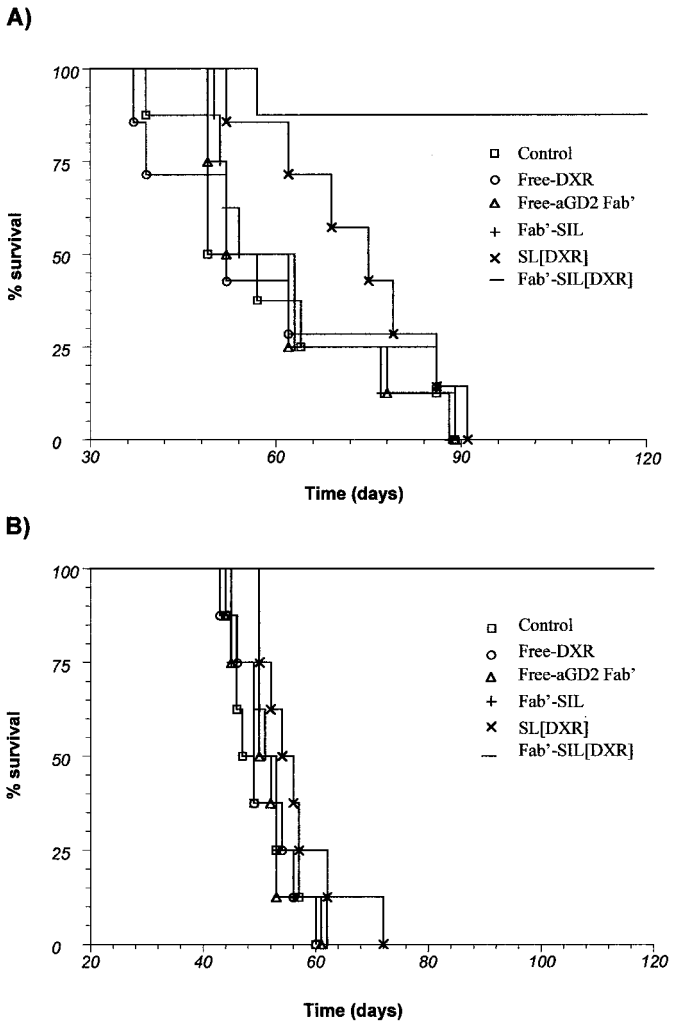

Fig. 4. Survival of tumor-bearing mice after various treatments. Treatment groups ($n = 8$/group) consisted of free-DXR (○), SL[DXR] (×), Fab′-SIL[DXR] (−), free-aGD$_2$ Fab′ (△), Fab′-SIL (+), and HEPES buffer (*control*, □). *A*, mice received injections in the tail vein with 3.5×10^6 HTLA-230 cells on day 0 and on days 1, 3, 5, and 7, mice received 2.5 mg/kg of DXR. *B*, mice received injections in the tail vein with 4×10^6 HTLA-230 cells on day 0, and 1 and 3 days postinoculation mice received 5 mg/kg of DXR. Four months after the beginning of the treatment, 100% of treated mice were still alive and showed a significant improvement ($P < 0.0001$) in survival times compared with free-DXR, SL[DXR], free-aGD$_2$ Fab′, Fab′-SIL, and HEPES buffer.

Fab′-SIL[DXR] selectively inhibited NB growth in all of the examined organs in nude mice (Table 2). Noteworthy, mice receiving Fab′-SIL[DXR] and schedule B (5 mg/kg DXR on days 1 and 3) were still alive after 4 months and could be considered cured ($P < 0.0001$).

Because in the previous experiments a few animals experienced reversible DXR toxicities, *e.g.*, weight loss and cutaneous toxicity, mice were treated with a single injection of Fab′-SIL[DXR] (10 mg DXR/kg) 1 day after tumor cell injection. All of these mice outlived the control mice by >5 months, with control mice dying from widespread metastatic disease ($P < 0.0001$; data not shown).

DISCUSSION

In this work we have shown that the anticancer drug DXR, when entrapped in aGD$_2$-immunoliposomes, can be selectively targeted to, and have preferential cytotoxicity for, GD$_2$-positive NB cells *in vitro*. Because a nontargeted, long circulating (Stealth) liposomal formulation of DXR (Doxil/Caelyx) is already approved for clinical use in the treatment of Kaposi's sarcoma and ovarian cancer (12, 13), we investigated whether it could be an effective treatment modality even for patients suffering from NB. Of particular significance to the clinical treatment of NB is our observation that complete inhibition of the metastatic growth of human NB cells in a xenograft model of nude mice was obtained by treating the tumor-bearing mice with this liposomal DXR targeted via aGD$_2$-Fab′.

The exposure of NB cells to aGD$_2$-SIL[DXR] resulted in a significantly greater inhibition of cell proliferation, *in vitro*, than that obtained for nontargeted liposomes. As expected, no differences in cell association and inhibition of cell proliferation were observed for aGD$_2$-targeted compared with nontargeted liposomal DXR on GD$_2$-negative cell lines. These results are compatible with the interpretation that binding and internalization of aGD$_2$-immunoliposomes contributed to the increased cytotoxicity of aGD$_2$-SIL[DXR] against GD$_2$-positive cells. Competition data provided an additional indication that aGD$_2$-SIL[DXR] internalization was receptor mediated, indicating that the ability of targeted liposomes to trigger receptor-mediated endocytosis is important for the cytotoxicity of their encapsulated drugs (20, 22, 32). These results are in agreement with previous reports showing that endocytosis of targeted immunoliposomes leads to release of drug from the internalized material into the cytosol and to subsequent cytotoxicity (17, 40–42).

Previous preclinical studies showed that lysis of NB cells by mouse and chimeric aGD$_2$ resulted from antibody-dependent cellular cytotoxicity and complement-depended cytotoxicity (7, 8, 38). Because we desired to avoid complicating the interpretation of our results by this nonspecific mechanism of cell kill, in the second part of our study we investigated a new therapeutic strategy, by using a liposomal carrier targeted by aGD$_2$ Fab′ fragments, which should allow us to obtain a therapeutic effect attributable primarily to the cytotoxic effect of entrapped DXR. The use of the Fab′ fragment of aGD$_2$ instead of whole mAb abolishes the mononuclear phagocyte system uptake of the aGD$_2$, which takes place via an Fc receptor-mediated mechanism (43). Moreover, it has been shown that small PEG immunoliposomes with Fab′ fragments coupled at the PEG terminus have significantly longer circulation time than comparable formulations containing whole mAbs (23). This can result in enhanced accumulation of the liposomes in solid tumor (23) and in significant suppression of tumor growth (24). Fab′-SIL, like aGD$_2$-SIL, showed specific cell association to GD$_2$-positive NB cells, but unlike aGD$_2$-SIL, were long-

Table 2 *Evaluation of NB metastases in nude/nude mice*

	Control	Free-DXR	Free-GD2 Fab′	Fab′-SIL	SL[DXR]	Fab′-SIL[DXR]
Ovaries	50–60[a]	60–70	40–50	60–60	50–60	0–10
Kidneys	50–50	50–60	40–50	50–50	50–60	0–10
Adrenal glands	30–40	20–30	20–30	30–40	30–40	0–0
Lymphonodes	40–40	20–30	30–40	30–30	20–30	0–0
Bone marrow	30–30	30–40	20–30	30–40	30–30	0–0
Spleen	0–10	10–10	0–10	0–10	0–10	0–0

[a] HTLA-230 3.5×10^6 were injected *i.v.* in *nu/nu* mice on day 0. On days 1, 3, 5, and 7, mice received 2.5 mg/kg mice weight of DXR, free or encapsulated in SL or Fab′-SIL. Free-GD2 Fab′, Fab′-SIL, and HEPES buffer (control) were also injected in mice. After 45 days the organs were surgically removed from the mice, fixed in 10% buffered formalin, processed for paraffin embedding, sectioned at 5–10 μm, and stained with H&E. The experiment (10 mice/group) was performed twice, and the data represent the percentage of microscopic metastases in each organ.

circulating, having MRTs almost identical to that obtained with nontargeted liposomes (SL). As shown previously (10, 44), long circulation times are required for liposomes to gain access to tumor sites.

The human NB cell line HTLA-230 was chosen for our investigation into the therapeutic efficacy of Fab′-SIL[DXR] because, when injected i.v. in nude mice, this xenograft model mimics the metastatic spread observed in advanced-stage NB patients (25). A number of studies conducted on large cohorts of patients have shown that the presence of circulating NB cells in the blood and micrometastases in the bone marrow at the time of primary surgery are strong predictors of relapse (45). Because bone marrow micrometastases are a direct measurement of the ability of tumor cells to spread systemically, the establishment of a model that closely mimics the clinical situation allows a more realistic evaluation of antitumor therapies. Thus, the experimental metastatic model used in these studies provides a consistent test for the potential use of targeted DXR in human metastatic disease. The schedule of treatment was chosen deliberately to allow for evaluation of the effects of treatments during the metastatic cascade, *i.e.*, during the stages in which tumor cells are in intravascular circulation and endothelium-attachment take place, or when extravasation, stromal invasion, and colonization take place (46, 47).

The efficacy of Fab′-SIL[DXR] was evaluated in terms of metastasis growth inhibition and increasing life span, which represent the principal end points for establishing the antitumoral activity of a new drug formulation. Keeping in mind that the highest dose of DXR that can be administered to nude mice is 10 mg DXR/kg weekly (39, 48), together with the considerations above, we designed a schedule in which mice received 5 mg DXR/kg on days 1 and 3 after inoculation of tumor cells. Using this protocol, 100% of mice treated with Fab′-SIL[DXR] were still alive >4 months after treatment ($P < 0.0001$ compared with control).

In conclusion, in this work we have shown significant improvements in the therapeutic effects of the chemotherapeutic drug DXR, when encapsulated in immunoliposomes targeted with the Fab′ of aGD_2. Long-term survival rates approaching 100% were observed for several doses and dosing schedules of the immunoliposomes, suggesting that total inhibition of the metastatic growth of human NB in a xenograft model of nude mice was occurring. Although Ahmad *et al.* (49) have demonstrated previously that immunoliposomes can partially eradicate lung cancer in a metastatic murine tumor model, it is important to emphasize that this is the first work, to our knowledge, in which it has been possible to completely prevent the growth of NB cells as macro- and micrometastases with the use of immunospecific liposomes. As a note of caution, SIL appear to lose their advantage when attempts are made to treat established advanced solid tumors (20, 35, 49), likely because the "binding site barrier" restricts penetration of SIL into the tumor (50, 51). It is our opinion that Fab′-SIL[DXR] deserve clinical evaluation as an adjuvant therapy for advanced-stage NB disease or for disease resulting from incomplete surgery or early micrometastatic lesions. Moreover, because other neuroectoderma-derived tumors, such as melanoma, express abundant amounts of the GD_2 epitope (18, 19, 52) use of these new targeted liposomal formulations of DXR may provide an effective therapeutic strategy for additional GD_2-positive human tumors.

ACKNOWLEDGMENTS

We thank Dr. Ralph A. Reisfeld for furnishing us with the hybridoma 14G.2a secreting a murine mAb of immunoglobulin G2a isotype subclass, specific for the GD_2 antigen; Dr. João N. Moreira and Susan Cubit for expert technical assistance, Dr. Claudio Gambini for histological evaluation, and Drs. Ralph A. Reisfeld, Paolo G. Montaldo, and V. Pistoia for helpful discussions.

REFERENCES

1. Maris, J. M., and Matthay, K. K. Molecular biology of neuroblastoma. J. Clin. Oncol., *17:* 2264–2279, 1999.
2. Niethammer, D., and Handgretinger, R. Clinical strategies for the treatment of neuroblastoma. Eur. J. Cancer, *31A:* 568–571, 1995.
3. Ladenstein, R., Philip, T., Lasset, C., Hartmann, O., Garaventa, A., Pinkerton, R., Michon, J., Pritchard, J., Klingebiel, T., Kremens, B., Pearson, A., Coze, C., Paolucci, P., Frappaz, D., Gadner, H., and Chauvin, F. Multivariate analysis of risk factors in stage 4 neuroblastoma patients over the age of one year treated with megatherapy and stem-cell transplantation: a report from the European Bone Marrow Transplantation Solid Tumor Registry. J. Clin. Oncol., *16:* 953–965, 1998.
4. Richardson, D. S., and Johnson, S. A. Anthracyclines in hematology: preclinical studies, toxicity and delivery systems. Blood Rev., *11:* 201–223, 1977.
5. Mujoo, K., Cheresh, D. A., Yang, H. M., and Reisfeld, R. A. Disialoganglioside GD_2 on human neuroblastoma cells: target antigen for monoclonal antibody-mediated cytolysis and suppression of tumor growth. Cancer Res., *47:* 1098–1104, 1987.
6. Schulz, G., Cheresh, D. A., Vark, N. M., Yu, A., Staffileno, L. K., and Reisfeld, R. A. Detection of ganglioside GD_2 in tumor tissues and sera of neuroblastoma patients. Cancer Res., *44:* 5914–5920, 1984.
7. Handgretinger, R., Anderson, K., Lang, P., Dopfer, R., Klingebiel, T., Schrappe, M., Reuland, P., Gillies, S. D., Reisfeld, R. A., and Neithammer, D. A phase I study of human/mouse chimeric antiganglioside GD2 antibody ch14.18 in patients with neuroblastoma. Eur. J. Cancer, *31A:* 261–267, 1995.
8. Uttenreuther-Fischer, M. M., Huang, C. S., and Yu, A. L. Pharmacokinetics of human-mouse chimeric anti-GD_2 mAb ch 14.18 in a phase I trial in neuroblastoma patients. Cancer Immunol. Immunother., *41:* 331–338, 1995.
9. Allen, T. M., Mehra, T., Hansen, C. B., and Chin, Y. C. Stealth liposomes: an improved sustained release system for 1-β-D-arabinofuranosylcytosine. Cancer Res., *52:* 2431–2439, 1992.
10. Gabizon, A., Catane, R., Uziely, B., Kaufman, B., Safra, T., Cohen, R., Martin, F., Huang, A., and Barenholz, Y. Prolonged circulation time and enhanced accumulation in malignant exudates of doxorubicin encapsulated in polyethylene-glycol coated liposomes. Cancer Res., *54:* 987–992, 1994.
11. Allen, T. M., Hansen, C. B., and Lopez de Menezes. D. E. Pharmacokinetics of long circulating liposomes. Adv. Drug Del. Rev., *16:* 267–284, 1995.
12. Northfelt, D. W., Martin, F. J., Working, P., Volberding, P. A., Russel, J., Newman, M., Amantea, M. A., and Kaplan, L. D. Doxorubicin encapsulated in liposomes containing surface-bound polyethylene glycol: pharmacokinetics, tumor localization, and safety in patients with AIDS-related Kaposi's sarcoma. J. Clin. Pharmacol., *36:* 55–63, 1996.
13. Muggia, F., Hainsworth, J. D., Jeffers, S., Miller, P., Groshen, S., Tan, M., Roman, L., Uziely, B., Muderspach, L., Garcia, A., Burnett, A., Greco, F. A., Morrow, C. P., Paradiso, L. J., and Liang, L. J. Phase II study of liposomal doxorubicin in refractory ovarian cancer: antitumor activity and toxicity modification by liposomal encapsulation. J. Clin. Oncol., *15:* 987–993, 1997.
14. Safra, T., Muggia, F., Jeffers, S., Tsao-Wei, D. D., Groshen, S., Lyass, O., Henderson, R., Berry, G., and Gabizon, A. Pegylated liposomal formulation of doxorubicin (doxil): reduced clinical cardiotoxicity in patients reaching or exceeding cumulative doses of 500 mg/m2. Ann. Oncol., *11:* 1029–1033, 2000.
15. Hansen, C. B., Kao, G. Y., Moase, E. H., Zalipsky, S., and Allen, T. M. Attachment of antibodies to sterically stabilized liposomes: evaluation, comparison and optimization of coupling procedures. Biochim. Biophys. Acta, *1239:* 133–144, 1995.
16. Ahmad, I., and Allen, T. M. Antibody-mediated specific binding and cytotoxicity of liposome-entrapped doxorubicin to lung cancer cells *in vitro*. Cancer Res., *52:* 4817–4820, 1992.
17. Pagnan, G., Stuart, D. D., Pastorino, F., Raffaghello, L., Montaldo, P. G., Allen, T. M., Calabretta, B., and Ponzoni, M. Delivery of c-myb antisense oligodeoxynucleotides to human neuroblastoma cells via disialoganglioside GD2-targeted immunoliposomes: antitumor effects. J. Natl. Cancer Inst., *92:* 253–261, 2000.
18. Pastorino, F., Stuart, D. D., Ponzoni, M., and Allen, T. M. Targeted delivery of antisense oligonucleotides in cancer. J. Control. Release, *74:* 69–75, 2001.
19. Pagnan, G., Montaldo, P. G., Pastorino, F., Raffaghello, L., Kirchmeier, M., Allen, T. M., and Ponzoni, M. GD2-mediated melanoma cell targeting and cytotoxicity of liposome-entrapped fenretinide. Int. J. Cancer, *81:* 268–274, 1999.
20. Lopez De Menezes, D. E., Pilarski, L. M., and Allen, T. M. *In vitro* and *in vivo* targeting of immunoliposomal doxorubicin to human B-cell lymphoma. Cancer Res., *58:* 3320–3329, 1998.
21. Moase, E. H., Qi, W., Ishida, T., Gabos, Z., Longenecker, B. M., Zimmermann, G. L., Ding, L., Krantz, M., and Allen, T. M. Anti-MUC-1 immunoliposomal doxorubicin in the treatment of murine models of metastatic breast cancer. Biochim. Biophys. Acta, *77996:* 1–13, 2000.
22. Park, J. W., Hong, K., Carter, P., Asgari, H., Guo, L. Y., Keller, G. A., Wirth, C., Shalaby, R., Kotts, C., Wood, W. I., Papahadjopoulos, D., and Benz, C. C. Development of anti-$p185^{HER2}$ immunoliposomes for cancer therapy. Proc. Natl. Acad. Sci. USA, *92:* 1327–1331, 1995.
23. Maruyama, K., Takahashi, N., Tagawa, T., Nagaike, K., and Iwatsuru, M. Immunoliposomes bearing polyethyleneglycol-coupled Fab′ fragment show prolonged circulation time and high extravasation into targeted solid tumours *in vivo*. FEBS Lett., *413:* 177–180, 1997.
24. Sugano, M., Egilmez, N. K., Yokota, S. J., Chen, F., Harding, J., Huang, S. K., and Bankert, R. B. Antibody targeting of doxorubicin-loaded liposomes suppresses the growth and metastatic spread of established human lung tumor xenografts in severe combined immunodeficient mice. Cancer Res., *60:* 6942–6949, 2000.
25. Bogenmann. E. A metastatic neuroblastoma model in SCID mice. Int. J. Cancer, *67:* 381–386, 1996.

26. Honsik, C. J., Jung, G., and Reisfeld, R. A. Lymphokine-activated killer cells targeted by monoclonal antibody to the disialoganglioside GD_2 and GD_3 specifically lyse human tumor cells of neuroectodermal origin. Proc. Natl. Acad. Sci. USA, *83:* 7983–7987, 1986.
27. Pagnan, G., Caridi, G., Montaldo, P. G., Bado, M., Chiesa, V., Allen, T. M., and Ponzoni, M. Apoptosis of human neuroblastoma cells induced by liposome-encapsulated fenretinide. J. Liposome Res., *8:* 401–423, 1998.
28. Olson, F., Hunt, C. A., Szoka, F. C., Vail, W. J., and Papahadjopoulos, D. Preparation of liposomes of defined size distribution by extrusion through polycarbonate membranes. Biochim. Biophys. Acta, *557:* 9–23, 1979.
29. Bolotin, E. M., Cohen, R., Bar, L. K., Ninio, E. S., Lasic, D. D., and Barenholz, Y. Ammonium sulphate gradients for efficient and stable remote loading of amphipathic weak bases into liposomes and ligandosomes. J. Liposome Res., *4:* 455–479, 1994.
30. Ponzoni, M., Bocca, P., Chiesa, V., Decensi, A., Pistoia, V., Raffaghello, L., Rozzo, C., and Montaldo, P. G. Differential effects of N-(4-hydroxyphenyl)retinamide and retinoic acid on neuroblastoma cells: apoptosis versus differentiation. Cancer Res., *55:* 853–861, 1995.
31. Mosmann, T. Rapid colorimetric assay for cellular growth and survival: application to proliferation and cytotoxicity assays. J. Immunol. Methods, *65:* 55–63, 1983.
32. Lopez De Menezes, D. E., Kirchmeier, M. J., Gagne, J. F., Pilarski, L. M., and Allen, T. M. Cellular trafficking and cytotoxicity of anti-CD19-targeted liposomal doxorubicin in B lymphoma cells. J. Liposome Res., *9:* 199–228, 1999.
33. Forssen, E. A., Male-Brune, R., Adler-Moore, J. P., Lee, M. J. A., Schmidt, P. G., Kraieva, T. B., Shimizu, S., and Tromberg, B. J. Fluorescence imaging studies for the disposition of daunorubicin liposomes (DaunoXome) in tumor tissue. Cancer Res., *56:* 2066–2075, 1996.
34. Sommermann, E. F., Pritchard, P. H., and Cullis, P. R. 125I labelled inulin: a convenient marker for deposition of liposomal contents *in vivo*. Biochim. Biophys. Res. Commun., *122:* 319–324, 1984.
35. Allen, T. M., Ahmad, I., Lopez De Menezes, D. E., and Moase, E. H. Immunoliposomes-mediated targeting of anti-cancer drugs *in vivo*. Biochem. Soc. Trans., *23:* 1073–1079, 1995.
36. Allen, T. M., and Hansen, C. Pharmacokinetics of stealth versus conventional liposomes: effect and dose. Biochim. Biophys. Acta, *1068:* 133–141, 1991.
37. Moreira, J. N., Hansen, C. B., Gaspar, R., and Allen, T. M. A growth factor antagonist as a targeting agent for sterically stabilized liposomes in human small cell lung cancer. Biochim. Biophys. Acta, *1514:* 303–317, 2001.
38. Yu, A. L., Uttenreuther-Fischer, M. M., Huang, C. S., Tsui, C. C., Gillies, S. D., Reisfeld, R. A., and Kung, F. H. Phase I trial of a human-mouse chimeric anti-disialoganglioside monoclonal antibody ch14.18 in patients with refractory neuroblastoma and osteosarcoma. J. Clin. Oncol., *16:* 2169–2180, 1998.
39. Fiebig, H. H., Berger, D. P., Winterhalter, B. R., and Plowman, J. *In vitro* and *in vivo* evaluation of US-NCI compounds in human tumour xenografts. Cancer Treat. Rev., *17:* 109–117, 1990.
40. Wang, S., Lee, R. J., Cauchon, G., Gorenstein, D. G., and Low, P. S. Delivery of antisense oligodeoxyribonucleotides against the human epidermal growth factor receptor into cultured KB cells with liposomes conjugated to folate via poly-ethylene glycol. Proc. Natl. Acad. Sci. USA, *92:* 3318–3322, 1995.
41. Lee, R. J., and Low, P. S. Folate-mediated tumor cell targeting of liposome-entrapped doxorubicin *in vitro*. Biochim. Biophys. Acta, *1233:* 134–144, 1995.
42. Kirpotin, D., Park, J. W., Hong, K., Zalipsky, S., Li, W. L., Carter, P., Benz, C. C., and Papahadjopoulos, D. Sterically stabilized anti-HER2 immunoliposomes: design and targeting to human breast cancer cells *in vitro*. Biochemistry, *36:* 66–75, 1997.
43. Tardi, P., Bally, M. B., and Harasym, T. O. Clearance properties of liposomes involving conjugated proteins for targeting. Adv. Drug Deliv. Rev., *32:* 99–118, 1998.
44. Papahadjopoulos, D., Allen, T. M., Gabizon, A., Mayhew, E., Matthay, K., Huang, S. K., Lee, K. D., Woodle, M. C., Lasic, D. D., Redemann, C., and Martin, F. J. Sterically stabilized liposomes: improvements in pharmacokinetics and antitumor therapeutic efficacy. Proc. Natl. Acad. Sci. USA, *88:* 11460–11464, 1991.
45. Moss, T., Reynolds, C. P., Sather, H. N., Romansky, S. G., Hammond, G. D., and Seeger, R. C. Prognostic value of immunocytologic detection of bone marrow metastases in neuroblastoma. N. Engl. J. Med., *324:* 219–226, 1991.
46. Al-Mehbi, A. B., Tozawa, K., Fisher, A. B., Shienag, L., Lee, A., and Mushel, R. J. Intravascular origin of metastasis from the proliferation of endothelium-attached tumor cells: a new model for for metastasis. Nat. Med., *6:* 100–102, 2000.
47. Chambers, A. F., Groom, A. C., and MacDonald, I. C. Dissemination and growth of cancer cells in metastatic sites. Nat. Rev. Cancer, *2:* 563–572, 2002.
48. Arap, W., Pasqualini, R., and Ruoslahti, E. Cancer treatment by targeted drug delivery to tumor vasculature in a mouse model. Science (Wash. DC), *279:* 377–380, 1998.
49. Ahmad, I., Longenecker, M., Samuel, J., and Allen, T. M. Antibody-targeted delivery of doxorubicin entrapped in sterically stabilized liposomes can eradicate lung cancer in mice. Cancer Res., *53:* 1484–1488, 1993.
50. Yuan, F., Leunig, M., Huang, S. K., Berk, D. A., Papahadjopoulos, D., and Jain, R. K. Microvascular permeability and interstitial penetration of sterically stabilized (stealth) liposomes in a human tumor xenograft. Cancer Res., *54:* 3352–3356, 1994.
51. Osdol, W. V., Fujimori, K., and Weinstein, J. N. An analysis of monoclonal antibody distribution in microscope tumour nodules: consequences of a " binding site barrier". Cancer Res., *51:* 4776–4784, 1991.
52. Cheresh, D. A., Harper, J. R., Schulz, G., and Reisfeld, R. A. Localization of the gangliosides GD_2 and GD_3 in adhesion plaque and on surface of human melanoma cells. Proc. Natl. Acad. Sci. USA, *81:* 5767–5771, 1984.

Doxorubicin-loaded Fab′ Fragments of Anti-disialoganglioside Immunoliposomes Selectively Inhibit the Growth and Dissemination of Human Neuroblastoma in Nude Mice

Fabio Pastorino, Chiara Brignole, Danilo Marimpietri, et al.

Cancer Res 2003;63:86-92.